# An Improved Method for Palladium Nanoparticles Detection on Carbon Materials in Scanning Electron Microscope Images

*M.Yu. Kurbakov [1], V.V. Sulimova [1], O.S. Seredin [1], A.V. Kopylov [1]*
*[1] Tula State University, 300012, Russia, Tula, Lenina Ave. 92*

***Abstract***

The subject of this paper is the urgent problem of detecting palladium nanoparticles on car-bon materials in grayscale scanning electron microscope images, the solution of which can be useful in many technological processes of the chemical industry. This is nontrivial problem and, currently, there is no method that would have all the necessary qualities for its solution.

This work is based on our previously developed method for detecting nanoparticles based on exponential approximation, which showed the best accuracy for scanning electron microscope images in absence of essential background irregularities. However, it has two significant shortcomings: 1) high demands on computing resources and 2) in the presence of background irregularities it produces a large number of false positives. This paper proposes a method that preserves the basic assumptions and general concept and, accordingly, the main advantages of earlier proposed approach, however, it contains a number of significant improvements that allow eliminating the above-mentioned shortcomings.

Experiments show that the proposed method reduces the number of false positives by 60-70% for SEM images with background irregularities while decreasing the nanoparticle detection time by approximately two to three times compared with the previously proposed approach.

Keywords: noisy image analysis, nanoparticle detection, exponential approximation with shift.

Citation: Kurbakov MY, Sulimova VV, Seredin OS, Kopylov AV. An Improved Method for Palladium Nanoparticles Detection on Carbon Materials in Scanning Electron Microscope Images. Computer Optics 2026; 50(3): 1825. doi: 10.18287/COJ1825.

## *Introduction*

Scanning electron microscopy (SEM) today is one of the most effective and advanced methods of studying the microstructure of solids [1]. In particular, it is used to solve the urgent problem of mapping "hidden" defects on the surface of carbon materials, which are extremely difficult to detect by other methods. Detection of defects is a critical step in many technological processes, since their presence affects the properties of catalytic activity and, consequently, the ability to accelerate chemical processes [2].

The mapping methodology involves applying metal nanoparticles (for example, 1 – 5 nm sized palladium nanoparticles) to the surface being studied as markers and then photographing it using an electron microscope [2]. A direct relationship between the presence of defects and the location of nanoparticles in an electron microscope image (SEM image) has been studied and experimentally proven in a number of works [3, 4].

However, the application of this methodology in practice is hampered by the lack of reliable and interpretable automatic methods for nanoparticles detection and consequent analyzing of its arrangement.

It should be noted that even the first task of detecting palladium nanoparticles on the surface of carbon materials, which is the subject of this work, is a non-trivial problem. Its solution is complicated by several circumstances: 1) grayscale SEM images that require analysis are usually very noisy and having uneven brightness, may contain overexposed areas and various structural elements of the material surface (background irregularities) that are not related to nanoparticles and defects; 2) nanoparticles are very small-sized (usually 1-4 dozen pixels) and can be located very close and even partially overlap each other; 3) a very small amount of expert-labeled data (essentially intended for quality assessment, not for training).

## *1. Related approaches*

Currently, there are many methods for detecting objects in images, which can be divided into two main groups: traditional computer vision methods, which are based on mathematical and statistical approaches, and deep learning neural network methods, which allow automatic extraction of features from images. However, none of the known methods satisfies all the requirements listed above.

The most common and simple method of detecting objects in an image, related to the category of computer vision methods, is threshold processing, for example, using binarization based on the adaptive Otsu threshold [5]. At that, as a rule, threshold processing allows us to determine only the approximate location of objects, and to clarify their coordinates and shape, it is necessary to use additional computer vision methods, such as an ellipse filter [6], circular Hough transform [7], specialized distance transformation with subsequent contour extraction [8], watershed segmentation [9, 10], local approximation of the brightness function by the exponential [11] or quadratic [12] model.

Methods of this group perform reasonably well in detecting non-intersecting objects of varying sizes and brightness, with clear boundaries and located against a relatively uniform background. However, their working quality significantly degrades in the case of the presence of a large number of "clumped" objects, significant background irregularities and high image noise (which is typical for the problem under consideration).

Noise sensitivity can be significantly reduced by image filtering. [11, 13] or the use of morphological operations to refine the shape of objects [14].

To solve the problem of uneven image brightness, a background subtraction method (e.g., rolling ball method) [12] or specialized adaptive filtering [11] can be used instead of simple threshold filtering.

To solve the problem of closely spaced or intersecting nanoparticles, the circular Hough transform [15] can be used for round particles or Canny boundary detection operator [16] for particles of arbitrary shape. However, these methods are inapplicable in the case of fuzzy boundaries and small particle sizes. In this case, local approximation methods are more suitable [11, 12].

Quite a large number of works are devoted to the detection of nanoparticles using neural network methods. In particular, methods are known for detecting large-sized (hundreds of pixels) non-overlapped nanoparticles for a simple background [17, 18, 19] and for very noisy images [20], for overlapped nanoparticles on a simple background [19, 21] and sometimes for small-sized nanoparticles [22]. However, the quality of nanoparticles detection by a neural network depends significantly on the availability of enough amount of training data, which is lacking in the considered case. Trying to solve the problem without enough training data leads to unsatisfactory results [23]. The only successful case of using a neural network for the problem of interest [3] consists in applying deep neural network only at the image segmentation stage combining it with additional methods to obtain nanoparticles centers and sizes.

Some works dealt with the detection problem in conditions of non-uniform background [15, 20, 24], but they are not suitable for detecting large numbers of small nanoparticles, and [15] also does not provide for the possibility of the overexposed areas existence.

Thus, the method we proposed earlier [11] best meets the listed requirements of the problem being solved. This method, based on a local approximation of the brightness function by an exponential model, demonstrated the best quality of detection of overlapped small-sized nanoparticles in conditions of highly noisy images compared to a number of other computer vision methods, as well as the neural network approach [3] on images that do not contain background irregularities.

However, during its further use, two very significant shortcomings were revealed: 1) it has high demands on computing resources and 2) in presence of image background irregularities it produces a large number of false positives.

## *2. Contribution of the paper*

This paper proposes a new method that preserves the basic assumptions and general concept and, accordingly, the main advantages of our earlier proposed approach [11], however, it contains a number of improvements, most significant of them are: 1) finding and excluding from the further consideration areas of background irregularities, 2) selecting small image fragments that are similar to nanoparticles based on finding local maxima to decrease the computational complexity of the method for images with small number of nanoparticles, 3) more effective computational procedure for image fragments approximation, 4) new criterion to determine whether a fragment contains a nanoparticle.

These improvements make it possible to eliminate the above-mentioned shortcomings. practically at all stages of the method that allow eliminating the above-mentioned shortcomings.

The experimental results show that the method proposed in this paper maintains approximately the same level of nanoparticles detection quality for SEM images without sufficient background irregularities, but at the same time allows for a significant reduction in the number of false positives (and, accordingly, an increase in the overall nanoparticles detection quality) for SEM images in the presence of background irregularities.

At the same time, the proposed method demonstrates significantly higher performance compared to the previously proposed approach.

## *3. Exponential approximation method for nanoparticles detection*

### 3.1. The main conception of the proposed approach

Following our previous approach to nanoparticles detection [11], new Exponential approximation method is based on two main assumptions:

- the visual representation of each nanoparticle in the image can be modeled quite well using the exponential brightness function with a maximum at the center of the nanoparticle;
- parameters of the approximating functions found for small image fragments will differ for fragments that contain and do not contain a nanoparticle.

The proposed method consists of the following stages: preprocessing (section 3.2), searching for areas of background irregularities (section 3.3), selecting basic small image fragments that are similar to nanoparticles (section 3.4), approximating the image fragments with the exponential model with offset with best local search around the basic fragment (sections 3.5 – 3.6), computing the radius of a hypothetical nanoparticle (section 3.7) and determining whether a fragment contains a nanoparticle (section 3.8).

### 3.2. Image preprocessing

In the context of the considered task of detecting palladium nanoparticles on carbon, SEM images obtained during the chemical experiments are noisy and may contain overexposed areas, which complicates the detection of nanoparticles. In this regard, the initial images require preliminary processing.

Following, we apply the median filtering to decrease image noise and then use the greyscale morphology method, namely the top-hat transform [25], to eliminate bright areas that exceed a given size. Fig. 1*a*, *b* shows the initial SEM image and the result of its preprocessing. As can be seen, the proposed preprocessing allows us to eliminate large overexposed areas, reduce image noise, and emphasize small bright areas.

### 3.3. Finding areas of background irregularities

As mentioned above, the method proposed in [11] produces many false positives in areas of SEM images that correspond to surface irregularities of the material. Such areas can be quite large and significantly decrease the overall nanoparticles detection quality.

To solve this problem, we propose a special, fairly simple way to detect such areas, which is based on the observation that they, as a rule, are quite large, are brighter than the background. Background irregularities areas can have various shapes. They often have the form of straight or broken lines, and in a number of cases can be arcuate.

Let $\boldsymbol{I} = \left[I_{i,j} = I(x_i, y_j), \quad i = 1, \ldots, N_x, j = 1, \ldots, N_y\right]$ be an image of size $N_x \times N_y$ with intensity values $I_{i,j}$ at the respective points $[x_i, y_j]$, that is obtained as the result of the preprocessing in accordance with the section 3.2.

To find background irregularity areas, first of all, we apply the normalization and gamma correction for each point $\tilde{I}_{i,j} = \left(I_{i,j} \times 255/I_{max}\right)^{\gamma}$, where $I_{max} = \max\limits_{i,j}\left(I_{i,j}\right)$ and $\gamma \in (0; 1]$. This transformation brings different images to a single brightness range and emphasizes bright areas, increasing their contrast with the background. Then simple (global) image thresholding to the transformed image $\tilde{I}_{i,j}$ is applied to obtain image areas with values exceeding the threshold $th_{ir}$: $A_k = \{(i,j): \tilde{I}_{i,j} \geq th_{ir}\}, \quad k = 1, \ldots, K$. Finally, large image areas, whose size exceeds the predefined threshold $|A_k| \geq asize$ are excluded from the consideration. In all experiments of this paper the constant parameters values are used: $\gamma = 0.4$, $th_{ir} = 100$ and $asize = 300$.

Fig. 1*c*-*f*, shows the intermediate stages of the finding areas of background irregularities on SEM image. The red dotted line roughly highlights the area that is excluded from the analysis as a result of this procedure.

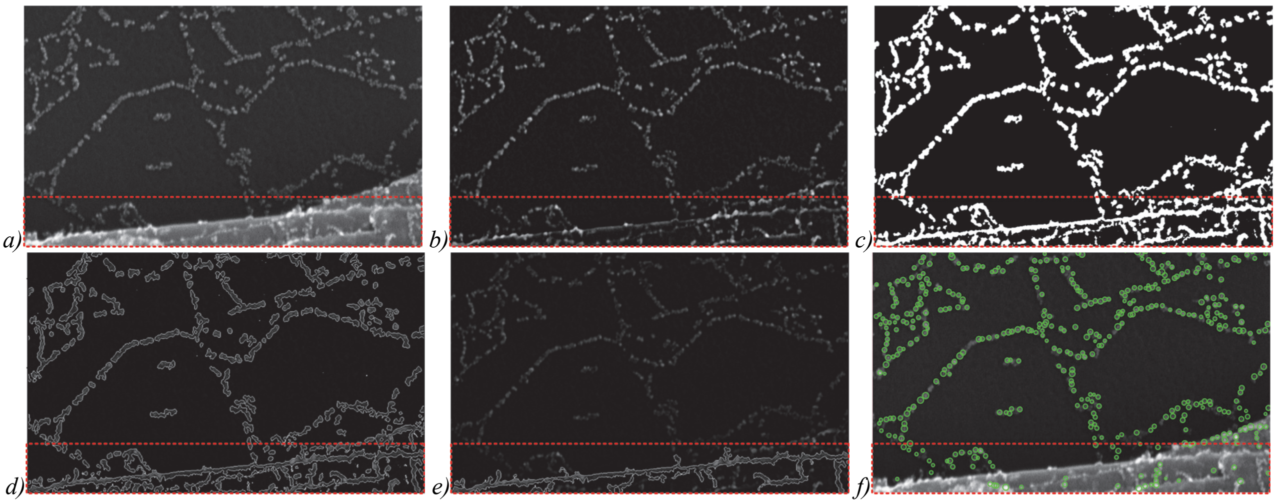


*Fig. 1. a) original SEM image, b) preprocessed SEM image, c) image after normalization, gamma correction, and threshold binarization, d) areas identified as a result of binarization, e) "background irregularities" – areas whose area exceeds the threshold, f) result of particle detection with the exclusion of areas of "background irregularities"*

### 3.4. Selecting basic small image fragments

Selecting basic small image fragments is made with the aim to decrease the computational complexity of the method by considering only those areas that are similar to nanoparticles. Paper [11] proposes to exclude form the consideration image fragments, whose brightness at the center point does not exceed the adaptive threshold that is computed over the full image.

In contrast to [11] in this paper we take as basic fragments only those ones, whose center points are local maxima of a preprocessed image. At that we consider only some finite number $L$ of largest local maxima points. Then these points are additionally filtered to exclude those of them that lie in background irregularity areas $|A_k| \geq asize$, found in accordance with the section 3.3.

Such preliminary filtering match the basic assumptions of the section 3.1, reduces the number of considered fragments and, respectively, the computing time in contrast to [11]. Also, at the same time it allows to increase in the overall nanoparticles detection quality due to excluding from the consideration fragments that lie in background irregularity areas.

### 3.5. Simple approximating one small image fragment with the exponential model with offset

Let $\boldsymbol{F} = \left[f_{ij} = f(x_i, y_j), \quad i,j = 1,\ldots, fsize\right]$ be a small image fragment, which has an odd size $fsize$. For each fragment, we used the same pixel coordinates $x_i, y_j \in \{-\lfloor fsize/2 \rfloor, \lfloor fsize/2 \rfloor\}$ and $i,j = 1,\ldots, fsize$ that are relative to the fragment center ($x_{\lfloor fsize/2 \rfloor} = 0, y_{\lfloor fsize/2 \rfloor} = 0$).

To approximate an image fragment, in contrast to [11] the exponential function with offset is used:

$$F(x,y,a,b,\Delta x,\Delta y) = a \cdot exp(-b \cdot [(x-\Delta x)^2 + (y-\Delta y)^2]). \quad (1)$$

Parameters $a > 0$ and $b > 0$ of the approximation function (1) define its width and height, respectively, and parameters $\Delta x, \Delta y \in \{-0.5, 0, 0.5\}$ define its offset along the corresponding axes.

The respective offset allows to made more accurate approximation (and later more accurate nanoparticle positioning) if the center of some nanoparticle is situated between image points.

Optimal values of unknown approximation parameters $a^{opt}, b^{opt}, \Delta x^{opt}, \Delta y^{opt}$of the exponential model (1) are determined in two steps.

At the first step nine pairs of optimal conditional parameter values $(a,b)^{opt}_{\Delta x,\Delta y}$ are determined for each of combinations $\Delta x, \Delta y \in \{-0.5, 0, 0.5\}$ as the decision of the optimization problem in accordance with the linearized least squares criterion:

$$J(x,y,a,b,\Delta x,\Delta y) = \sum_{i,j}\left[\ln F\left(x_i,y_j,a,b,\Delta x,\Delta y\right) - \ln f_{ij}\right]^2 = \sum_{i,j}\left[\ln a - b(x-\Delta x)^2 - b(y-\Delta y)^2 - \ln f_{ij}\right]^2. \quad (2)$$

$$(a,b)^{opt}_{\Delta x,\Delta y} = \underset{a,b}{\operatorname{argmin}} J(x,y,a,b,\Delta x,\Delta y), \quad \forall \Delta x, \Delta \mathrm{y} \in \{-0.5, 0, 0.5\}. \quad (3)$$

The optimization problem (3) has the unique solution that can be directly found by the formulas:

$$\begin{cases} b^{opt}_{\Delta x,\Delta y} = \left[\sum_{i,j} \ln f_{ij} \cdot \sum_{i,j} s_{ij} - n^2 \cdot \sum_{i,j} \ln f_{ij} \cdot s_{ij}\right] / \left[n^2 \cdot \sum_{i,j} s_{ij}^2 - \left(\sum_{i,j} s_{ij}\right)^2\right], \\ \qquad a^{opt}_{\Delta x,\Delta y} = \exp\left(\left(b^{opt}_{\Delta x,\Delta y} \cdot \sum_{i,j} s_{ij} + \sum_{i,j} \ln f_{ij}\right)/n^2\right), \end{cases} \quad (4)$$

where $s_{ij} = (x_i - \Delta x)^2 + (y_j - \Delta y)^2$, $n = fsize$ and if $f_{ij} = 0 \rightarrow \ln f_{ij} = 0$ is insufficient image fragment correction to ensure the correctness of the logarithm calculation.

At the second step the optimal offset is determined as the result of optimization of the normalized residual error:

$$E(a,b,\Delta x,\Delta y) = \sqrt{\sum_{i,j}\left[F\left(x_i,y_j,a,b,\Delta x,\Delta y\right) - f_{ij}\right]^2/n} \Bigg/ \left(\sqrt{\sum_{i,j} f_{ij}^2/n} + \sqrt{\sum_{i,j}\left[F\left(x_i,y_j,a,b,\Delta x,\Delta y\right)\right]^2/n}\right). \quad (5)$$

$$(\Delta x, \Delta \mathrm{y})^{opt} = \underset{\Delta x,\Delta \mathrm{y}}{\operatorname{argmin}} E\left(a^{opt}_{\Delta x,\Delta y}, b^{opt}_{\Delta x,\Delta y}, \Delta x, \Delta y\right). \quad (6)$$

The optimal offset $(\Delta x, \Delta y)^{opt}$ uniquely defines the respective optimal parameters $(a,b)^{opt}$.

As a result of this simple enough computing procedure, we have the full set of optimal parameter values $(a,b,\Delta x,\Delta y)^{opt}$ of the exponential model (1).

### 3.6. Best local approximation search

It should be noticed, that though brightness local maxima are good enough candidates to be centers of nanoparticles, but due to strong image noise they can be shifted respectively to these centers.

Exponential model with offset (section 3.5) allows to decide this problem if the mismatch of a local maxima and a nanoparticle center does not exceed 0.5 pixels (if a real nanoparticle center lies between pixels). The procedure of this section allows to detect a nanoparticle if there is a stronger shift of the local maximum.

The proposed procedure is simple enough. It consists in: 1) considering additional image fragments from some neighborhood of a local maximum, 2) applying for each of them the proposed simple exponential approximation with offset and 3) taking the best approximation result that delivers the minimum of the normalized residual error (5).

### 3.7. Computing radius of a nanoparticle

The radius of a nanoparticle for some image fragment is defined by the respective optimal value $b^{opt}$ as follows: $r = 1/\sqrt{b^{opt}}$.

### 3.8. Determining whether a fragment contains a nanoparticle

To determine whether some image fragment contains a nanoparticle or not the thresholding scheme is used. In the accordance with the proposed approach three main thresholds can be used:

1). the simple error threshold $th_{er}$ limits the normalized approximation error (5) that can be observed if the fragment contains a nanoparticle,

2). the adaptive threshold $th_a$ that sets the minimum acceptable value of the approximation parameter $a^{opt}$ in the used exponential model (1) for a fragment that contains a nanoparticle. This threshold is determined as the mean value of $N$ largest local maxima $LM_i, i = 1, \dots, N$ of the preprocessed image, multiplied by the positive coefficient $c_a \in [0,1]$:

$$th_a = c_a \cdot \sum_{i=1}^{N} LM_i / N, \tag{7}$$

3). the threshold $th_r$ that limits the radius of a nanoparticle.

So, fragment $\boldsymbol{f}$ contains a nanoparticle, if the condition $[(E(\boldsymbol{f}) \le th_{er})$ and $(a^{opt}(\boldsymbol{f}) \ge th_a)$ and $(r(\boldsymbol{f}) \le th_r)]$ holds true.

For all experiments of this paper the value of $N$ is set in 1000, i.e. the threshold (7) is determined over 1000 largest local maxima. This value should be corresponded to the order of nanoparticles quantity at the image. Thus, for several thousand nanoparticles, a more appropriate value is 1000, for several hundred it is equal to 100.

### *4. Detection quality evaluation*

The nanoparticles detection quality is determined here by comparing the detection results with expert nanoparticles labeling, that was made manually at the Digimizer image analysis software.

The result of detecting, as well as the result of expert labeling gives a set of circles, each of which is described by the coordinates of its center and the radius, which defines the size of the nanoparticle.

To assess the correctness of determining the position and size of the nanoparticle found by the algorithm, we used a method based on the calculation of the Jaccard measure between circles:

$$Jac(S_{gt}, S_{dt}) = |S_{gt} \cap S_{dt}| / |S_{gt} \cup S_{dt}|, \tag{8}$$

where $S_{gt}$ is the ground truth circle labeled by the expert, and $S_{dt}$ is the circle found by the detection algorithm. The greater the value of this measure, the smaller the difference between the object found by the algorithm and that manually labeled. When the value is equal to one, the found areas completely coincide.

In this work the value of the Jaccard measure, at which the corresponding nanoparticle is considered as found by the algorithm, is 0.25. More detailed description of computing and using the measure (8) can be found in [11].

The quality of the algorithms was evaluated by the accuracy value, which is calculated by the formula

$$accuracy = \frac{TP}{TP+FN+FP}, \tag{9}$$

where $TP$ is the number of particles correctly identified by the algorithm, i.e., matching with the expert markup with the Jaccard measure grater or equal than 0.25; $FN$ is the number of particles not found by the algorithm but labeled by the expert; and $FP$ is the number of particles found by the algorithm but not confirmed by the expert.

### *5. Experiments*

#### *5.1. Characteristics of the computing system and dataset*

An experimental study of the proposed method s was carried out on the computing systems with the next main characteristics: CPU – Intel Core i7-9700k, RAM – 16 Gb, OS – Windows 10x64.

Image dataset includes six SEM images of Pd/C catalysts from the public dataset [26]. These SEM images were obtained using a field-emission scanning electron microscope (FE-SEM) Hitachi SU8000 at 100x magnification. The operation conditions involved secondary electron mode at an accelerating voltage of 10-30 kV and an operating distance of 6-12 mm. The SEM images were acquired in TIFF format with a 1280 × 890 resolution.

#### *5.2. Study of nanoparticles detection quality in the absence of sufficient background irregularities*

First of all, we repeat here the experiment of our previous paper [11] to compare the proposed improved method in quality with its old version and with other methods for SEM images that do not contain sufficient structural irregularities of the material surface. The following methods were compared, for each of which preprocessed SEM images (section 3.2) were used as input data (except for Deep Neural Network):

1). Local Maxima [27] – method that takes local intensity maxima of SEM image exceeding some threshold as nanoparticle position, at that radius of all nanoparticle are taken the same and equal to the average size of the nanoparticle on the image of the given scale.

2). The Morphological Reconstruction [28] method is a powerful tool for object extraction based on markers and masks. Unlike basic morphological operations, it preserves object shapes while eliminating noise and restoring boundaries.

3). The Watershed Segmentation [29] method is an image technique based on a topographic metaphor. It treats an image as a topographic surface where pixel intensity represents elevation. The algorithm simulates flooding from local minima, with boundaries forming where different flood basins meet – these boundaries become the segmentation lines.

4-6) Feature detection methods based on second derivative analysis: Laplacian of Gaussian method [30], Difference of Gaussians method [31], based on a scale-normalized Determinant of the Hessian method [30]. The core idea involves searching for blob-structures – local regions with brightness distinct from the background.

7) Deep Neural Network approach described in [32] is focused on the problem of particle segmentation in SEM images. For training, 11 full-sized SEM images were manually labeling by expert and additional images obtained as a result of augmentation according to [32].

8) Previously proposed version of the Exponential Approximation method, developed by us in [11].

9) Improved Exponential Approximation method, proposed in this paper.

The experimental setup includes four manually labeled fragments of SEM images from the public dataset (section 5.1). Image fragments to be analyze contain about 200 expertly labeled nanoparticles per image, have no essential irregularities of the material surface.

To model the real situation in case of limited data amount we chose parameters of each algorithm based on the leave-one-out procedure [33]. Namely, four times in a turn, we selected one of the four images as the test image, found the set of parameters that gives the best sum of accuracies for the three remaining images, and applied this set to process the test image. Thus, the average accuracy for four test images provides the final estimation of the algorithm performance.

Unchangeable parameters of the proposed method, the same for all images and all runs within the given experiment: median filtering parameter $sz_{med} = 3$, top-hat parameter $sz_{th} = 4$, small image fragment size $fsize = 7$, the number of greatest local brightness maxima $L = 300$, $th_r = 5$ and the minimal distance between two local maximums is equal to 2.

As a leave-one-out result two parameters for the final filtering are chosen (section 3.8): the coefficient $c_a$ for the adaptive threshold $th_a$ (7) and the threshold for the normalized approximation error $th_{er}$. All parameters and the results of the other methods exactly repeat those of the paper [11].

The results of this experiment are presented at the Tab. 1. All the results were obtained for the object acceptability threshold equal to 0.25 according to the Jaccard measure (8). The central columns of the Tab. 1 contain accuracy values (in %) obtained for each image in accordance with the described leave-one-out procedure. The last column contains the average accuracy values and the corresponding standard deviations (SD) calculated from all four test images. The optimal parameter values that achieve the maximum overall accuracy for all four labeled image fragments from the experiment: $c_a = 0.27$ and $th_r = 0.32$.

*Tab. 1. Accuracies of nanoparticle detection for images without irregularities of the material surface*

| **Method** | **Images to find parameters/to test** | | | | **Mean ± SD** |
|---|---|---|---|---|---|
| | **2,3,4/1** | **1,3,4/2** | **1,2,4/3** | **1,2,3/4** | |
| **1. Local Maxima** | 73.90 | 67.52 | 69.92 | 73.33 | 71.16 ± 2.60 |
| **2. Morphological Reconstruction** | 45.28 | 48.02 | 57.21 | 72.92 | 55.86 ± 10.8 |
| **3. Watershed Segmentation** | 54.92 | 61.69 | 64.23 | 82.91 | 65.94 ± 10.4 |
| **4. Laplacian of Gaussian** | 58.44 | 64.47 | 70.52 | 80.30 | 68.43 ± 8.07 |
| **5. Difference of Gaussians** | 64.98 | 69.06 | 75.55 | 70.18 | 69.94 ± 8.36 |
| **6. Determinant of Hessian** | 39.08 | 47.71 | 48.33 | 70.82 | 51.48 ± 11.7 |
| **7. Deep Neural Network** | 69.88 | 67.95 | 76.09 | 79.59 | 73.38 ± 4.68 |
| **8. Exponential Approximation (OLD)** | 73.75 | 72.93 | 75.58 | 83.48 | 76.44 ± 4.81 |
| **9. Exponential Approximation (NEW)** | 73.66 | 74.29 | 76.36 | 82.51 | 76.71 ± 4.04 |

As we can see from the Tab. 1, for the considered set of images the obtained mean accuracy of the proposed in this paper method (NEW) slightly exceeds the accuracy of the previously proposed approach (OLD) and essentially outperforms other methods, including deep neural network. At the same time, it should be noted, that the standard deviation for NEW approach has been significantly decreased in contrast to the previous version. So, the proposed method is more stable to parameter changes compared to the previous approach as well as to practically all other methods under consideration.

## *5.3. Study of nanoparticles detection quality in the presence of background irregularities*

The main purpose of the experiment of this section consists in to compare the nanoparticles detection quality of the proposed in this paper approach and the quality of the method of exponential approximation [1] for SEM images with sufficient background irregularities.

For this purpose, two images labeled by an expert were used. These images are typical examples of palladium on carbon SEM images with background irregularities of different kind.

For each of these example images two methods have been applied: the exponential approximation method (OLD), proposed in [11] and its improved version, proposed here at the section 3.

Two ways of choosing changeable parameters for both methods were tested: 1) best parameters, that possess the maximum accuracy value and 2) parameters that possess the maximum summary accuracy for all four labeled image fragments from the experiment of the section 5.2.

Fig. 2 shows example images and results of nanoparticles detection, obtained for best parameters for each method. Blue circles at these figure are nanoparticles labeled by an expert that have been matched with the Jaccard measure 0.25 (section 4) to nanoparticles that have been found by the algorithm, which are in turn depicted by the green circles and are considered True Positives (*TP*). Red circles show nanoparticles that have been labeled by the expert, but have been not detected by the algorithm, i.e. False Negatives (*FN*). And, finally, False Positives (*FP*), i.e. detected nanoparticles that have not been accepted by the expert are depicted by yellow.

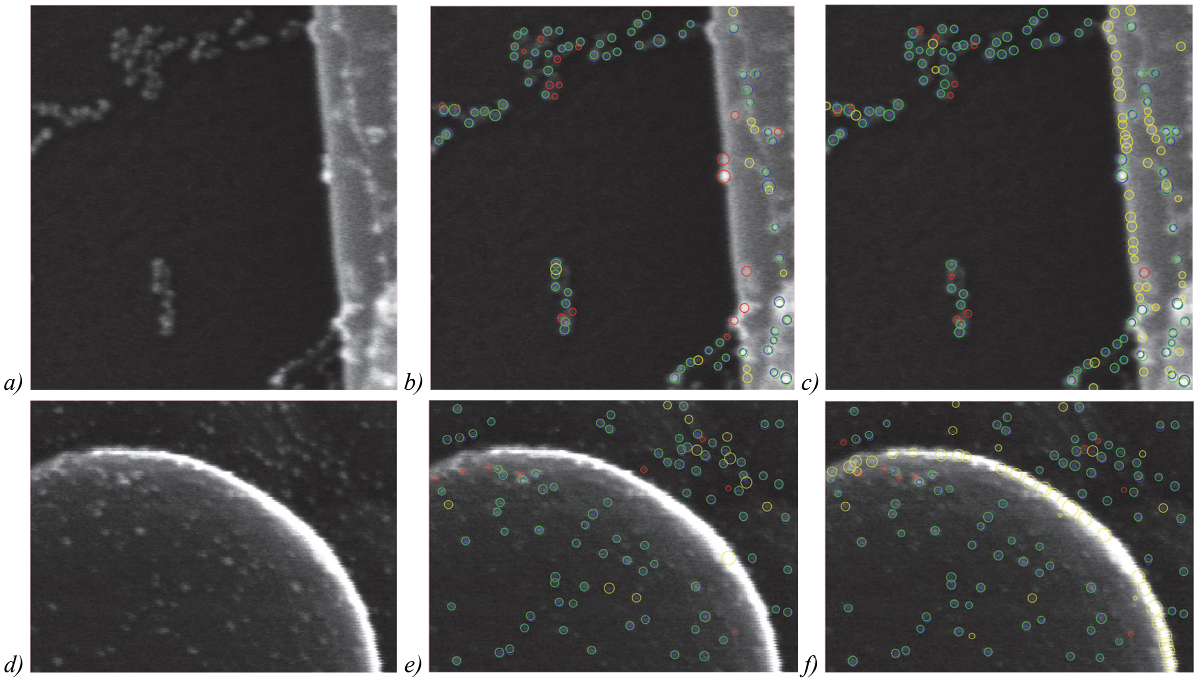

*Fig. 2. (a), (d) SEM image fragments with background irregularities; (b), (e) nanoparticle detection results for an improved version of the approach (NEW); (c), (f) nanoparticle detection results for previously proposed method (OLD)*

Tab. 2 presents the obtained accuracy values (and the respective TP, FN and FP values in parentheses) for both ways of parameters choosing.

*Tab. 2. Accuracies (and the respective TP, FN and FP values) for two ways of parameters choosing*

| **Method** | **Fig 2a** | | **Fig 2d** | |
|---|---|---|---|---|
| | **Best params** | **Estimated params** | **Best params** | **Estimated params** |
| **OLD** | 57.89 (77, 11, 45) | 55.94 (80, 8, 55) | 62.40 (78, 9, 38) | 56.64 (81, 6, 56) |
| **NEW** | 70.47 (74, 14, 17) | 66.67 (76, 12, 26) | 80.61 (79, 8, 11) | 76.09 (70, 17, 5) |

As we can see, the numerical results confirm superiority of the NEW method that allowed to increase the nanoparticles detection accuracy for the first image from 57.89 and for the second image – from 62.40 to 80.61 for best parameters values. For parameter values, that were estimated over other images ($c_a = 0.27$, $th_{er} = 0.32$ for NEW method and $Cf_{prep} = 0.3$, $Cf_{detect} = 0.4$ for OLD method), the accuracy, as expected, is slightly less the best possible accuracy. At that it should be noted, the proposed method reaches the better accuracy in contrast to the OLD method even for its best parameters values.

Thus, the visual and numerical results confirm that the method proposed in this paper allows to significantly reduce the number of false positives for images with background irregularities and thereby improve the overall nanoparticles detection accuracy.

### 5.4. Performance study

For the experimental performance study, 3 images with significantly different amounts of nanoparticles were selected (Fig. 3).

Tab. 3 contains mean times in seconds (averaged through 3 runs) and a number of nanoparticles (*N*) detected by the OLD method proposed in [11] and by its improved NEW version proposed in this paper.

Since the performance and nanoparticles detection result of the proposed method depend on the number of largest local maxima $L$ specified as a parameter (section 3.4), then in Tab. 2 one result of the OLD method corresponds to a series of results of the NEW method for a different $L$ values from 1000 to 4000. All results have been obtained in accordance with previous experiments. The parameters of the proposed method are divided into two groups, and their values were set based on section 5.2.

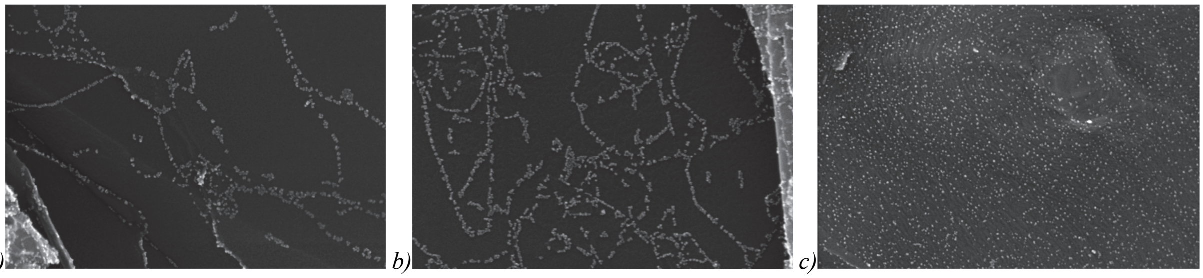

a) b) c)

*Fig. 3. SEM images for the experimental performance study with different numbers of nanoparticles*

*Tab. 3. Mean times (in seconds) and amount of nanoparticles detected by OLD and NEW methods*

| **Method** | | **Fig 3a** | | **Fig 3b** | | **Fig 3c** | |
|---|---|---|---|---|---|---|---|
| | | **Time** | ***N*** | **Time** | ***N*** | **Time** | ***N*** |
| **OLD** | | **91.00** | **1500** | **118.0** | **2500** | **112.0** | **3300** |
| **NEW** (for different *L*) | 1000 | 10.81 | 793 | 9.51 | 928 | 17.69 | 973 |
| | 1300 | 14.33 | 1015 | 12.61 | 1191 | 21.45 | 1262 |
| | 1600 | 16.76 | 1191 | 15.35 | 1458 | 26.19 | 1551 |
| | 1900 | 19.73 | 1264 | 18.61 | 1707 | 30.09 | 1839 |
| | 2200 | 23.01 | 1264 | 21.69 | 1946 | 35.77 | 2121 |
| | 2500 | 26.55 | 1264 | 29.84 | 2148 | 40.09 | 2408 |
| | 2800 | 29.84 | 1264 | 28.59 | 2262 | 44.73 | 2697 |
| | 3100 | 33.47 | 1264 | 32.48 | 2270 | 49.21 | 2985 |
| | 3400 | 37.15 | 1264 | 35.78 | 2270 | 54.10 | 3206 |
| | 3700 | 40.73 | 1264 | 39.53 | 2270 | 55.79 | 3262 |
| | 4000 | 45.04 | 1264 | 43.47 | 2270 | 59.36 | 3265 |

As can be seen from Tab. 3, the number of nanoparticles detected by the proposed method NEW increases with the $L$ value up to a certain limit, which corresponds to the number of nanoparticles in the image. Obviously, to detect all nanoparticles, it is necessary that the specified $L$ value exceed their expected number with some reserve.

This circumstance does not present a practical problem, since it does not require an accurate assessment of the number of nanoparticles and with an increase in the $L$ value, the operating time of the NEW method increases linearly and relatively insignificantly.

Table 3 also shows that the NEW method will detect approximately the same number of nanoparticles as the OLD method, but in a significantly shorter time. At that It should be noted that the difference in the number of detected nanoparticles is primarily explained by the significantly higher number of false positives in the OLD method compared to NEW.

The greatest effect from the application of the proposed method in terms of increasing productivity is observed with a small number of nanoparticles in the image. Increasing the number of nanoparticles requires increasing the $L$ value and, accordingly, leads to an increase in the running time of the NEW method.

However, as can be seen from the examples given, even for the case of a very dense nanoparticles arrangement (Fig. 3), the operating time of the NEW method is significantly lower than the operating time of the OLD method.

## *Discussions*

The proposed method is aimed at the automatic detection of small, approximately uniform-sized nanoparticles (1-4 dozen points of area) in grayscale images under conditions of high noise, uneven brightness, the presence of overexposed areas of various shapes and sizes, and background irregularities in the form of straight, broken, and curved lines of varying lengths and orientations related to the material surface features.

It is assumed that the nanoparticles have a spherical shape and are quite well approximated by an exponential function. They can be located either separately from each other or form conglomerates of closely located and even partially overlapping nanoparticles.

The method was originally developed for detecting light nanoparticles on a darker background, but can also be used for detecting dark nanoparticles on a light background after image inversion and if the assumptions specified in section 3.1 (about the exponential nanoparticles modeling) are met.

The method has a number of parameters, most of which can be set to default values suitable for processing most images that match the description above. Specifically, such default values are: median filtering parameter $sz_{med} = 3$, top-hat parameter $sz_{th} = 4$, maximum nanoparticle radius $th_r = 5$, small image fragment size $fsize = 7$ and the minimum distance between two local maximums is equal to 2.

However, there are several parameters whose values should be selected based on the available a priori information.

In particular, the parameter defining the number of greatest local brightness maxima *L* (section 3.4) used to find base image fragments potentially containing nanoparticles should be chosen in accordance with the expected number of nanoparticles in the image, adding some reserve to the upper estimate for the number of nanoparticles (which can range from several hundreds to a thousand local maxima, depending on the degree of confidence in the estimate used).

Experiment in section 5.4 demonstrates the dependence of the number of detected nanoparticles and the method's execution time on the value of this parameter. The experimental results show that, starting from a certain value of $L$, the number of detected nanoparticles stabilizes (i.e., taking into account additional local maxima does not lead to the detection of new nanoparticles), but it does increase the algorithm's execution time. Therefore, this parameter is convenient for reducing the method's execution time if a priori information about the approximate number of nanoparticles in the image is available. For fully automated data processing, a promising area of future research is the development of an adaptive criterion for the selection of $L$, for example, based on the stabilization of the number of detected nanoparticles. The performance improvement is particularly noticeable for small numbers of nanoparticles, but can also be noticeable for images with high nanoparticle densities.

Two other parameters requiring selection of values are the coefficient $c_a$, which determines the adaptive threshold for rejecting fragments that do not contain nanoparticles based on the brightness information at the fragment center, and the maximum allowable value of the normalized approximation error $th_{er}$. The optimal values of these two parameters may differ for different images. However, the experimental study (sections 5.2 and 5.3) conducted in this paper shows that sufficiently good estimates of these parameters values can be obtained based on the analysis of some number of labeled images with subsequent use of the obtained values for new images not involved in training.

The processing of images of different scales obtained at different magnifications is beyond the scope of this article. Clearly, at higher magnifications, the nanoparticles in the image will be larger, while at lower magnifications, they will be smaller. The method can be applied in this case with minor adjustments to the parameter values – the image fragment values and size filtering thresholds should correspond to the size of nanoparticles. An alternative method is to pre-convert the images to the desired scale. This approach was successfully applied in [34] when processing a complete database [26] of images of different scales using the OLD method [11]. Clearly, the same approach can be applied to its improved NEW version proposed in this paper.

As directions for further development of the proposed method, one can indicate its adaptation for processing images containing nanoparticles of significantly different sizes, as well as those having an elongated shape, which is not provided for in the current formulation of the method.

### *Conclusions*

In this paper proposes an improved method for nanoparticles detection in SEM images has been proposed. It preserves the basic assumptions and general concept and, accordingly, the main advantages of earlier proposed approach [11], however, it contains a number of significant improvements that allow eliminating its main shortcomings.

The experimental results show that the method proposed in this paper maintains approximately the same level of nanoparticles detection quality for SEM images without sufficient background irregularities, but at the same time allows for a significant reduction in the number of false positives (and, accordingly, an increase in the overall nanoparticles detection quality) for SEM images in the presence of background irregularities.

At the same time, the proposed method demonstrates significantly higher performance compared to the previously proposed approach.

### *Acknowledgements*

This research is funded by the Ministry of Science and Higher Education of the Russian Federation within the framework of the state task FEWG-2024-0001. The authors thank the Scientific School of Academic V.P. Ananikov for the research topic, useful discussions and provided experimental data.

### *References*

[1] Morishita K, Takarada T. Scanning electron microscope observation of the purification behaviour of carbon nanotubes. J Mater Sci 1999; 34(5): 1169-1174. doi:10.1023/A:1004544503055.

[2] Pentsak EO, Kashin AS, Polynski MV, Kvashnina KO, Glatzel P, Ananikov VP. Spatial imaging of carbon reactivity centers in Pd/C catalytic systems. Chem Sci 2015; 6(6): 3302-3313. doi:10.1039/C4SC00232F.

[3] Boiko DA, Pentsak EO, Cherepanova VA, Gordeev EG, Ananikov VP. Deep neural network analysis of nanoparticle ordering to identify defects in layered carbon materials. Chem Sci 2021; 12(25): 7428-7441. doi:10.1039/D0SC05696K.

[4] Fei Z, Rodin AS, Gannett W, et al. Electronic and plasmonic phenomena at graphene grain boundaries. Nat Nanotechnol 2013; 8(11): 821-825. doi:10.1038/nnano.2013.197.

[5] Otsu N. A threshold selection method from gray-level histograms. IEEE Trans Syst Man Cybern 1979; 9(1): 62-66. doi:10.1109/TSMC.1979.4310076.

[6] Groom DJ, Yu K, Rasouli S, Polarinakis J, Bovik AC, Ferreira PJ. Automatic segmentation of inorganic nanoparticles in BF TEM micrographs. Ultramicroscopy 2018; 194: 25-34. doi:10.1016/j.ultramic.2018.06.002.

[7] Kaya E, Kaya O, Alkan G, Gürmen S, Stopic S, Friedrich B. New proposal for size and size-distribution evaluation of nanoparticles synthesized via ultrasonic spray pyrolysis using search algorithm based on image-processing technique. Materials 2020; 13(1): 38. doi:10.3390/ma13010038.

[8] Vippola M, Valkonen M, Sarlin E, Lepistö T. Insight to nanoparticle size analysis: novel and convenient image analysis method versus conventional techniques. Nanoscale Res Lett 2016; 11: 169. doi:10.1186/s11671-016-1391-z.
[9] Wu Y, Wang W, Zhang F, Xiao Z, Wu J, Geng L. Nanoparticle size measurement method based on improved watershed segmentation. In: Proc 2018 Int Conf Electronics and Electrical Engineering Technology (EEET 2018); 2018. pp. 232-237. doi:10.1145/3277453.3286087.
[10] Slater TJA, Wang YC, Leteba GM, Quiroz J, Camargo PHC, Haigh SJ, Allen CS. Automated single-particle reconstruction of heterogeneous inorganic nanoparticles. Microsc Microanal 2020; 26(6): 1168-1175. doi:10.1017/S1431927620024642.
[11] Boiko DA, Sulimova VV, Kurbakov MY, Kopylov AV, Seredin OS, Cherepanova VA, Pentsak EO, Ananikov VP. Automated recognition of nanoparticles in electron microscopy images of nanoscale palladium catalysts. Nanomaterials 2022; 12(21): 3914. doi:10.3390/nano12213914.
[12] Shvedchenko DO, Suvorova EI. Combination of thresholding and fitting methods for measuring nanoparticle sizes and size distributions in (S)TEM. Microsc Res Tech 2017; 80(10): 1113-1122. doi:10.1002/jemt.22908.
[13] Nesterenko DV. Formation and processing of electron microscopic images. Comput Opt 2011; 35(2): 166-174.
[14] Kimori Y. Morphological image processing for quantitative shape analysis of biomedical structures: effective contrast enhancement. J Synchrotron Radiat 2013; 20(6): 848-853. doi:10.1107/S0909049513020761.
[15] Mirzaei M, Rafsanjani HK. An automatic algorithm for determination of the nanoparticles from TEM images using circular Hough transform. Micron 2017; 96: 86-95. doi:10.1016/j.micron.2017.02.008.
[16] Kook S, Zhang R, Chan Q, Aizawa T, Kondo K, Kudo H, Sako T. Automated detection of primary particles from transmission electron microscope images of soot aggregates in diesel engine environments. SAE Int J Engines 2016; 9(1): 279-296. doi:10.4271/2015-01-1991.
[17] López Gutiérrez JD, Abundez Barrera IM, Torres Gómez N. Nanoparticle detection on SEM images using a neural network and semi-synthetic training data. Nanomaterials 2022; 12(11): 1818. doi:10.3390/nano12111818.
[18] Luan X, Zhou Y, Tan X, Wang X, Mei X, Han X. Particle image detection based on Mask R-CNN combined with edge segmentation. J Appl Opt 2023; 44(1): 93-103. doi:10.5768/JAO202344.0102005.
[19] Wang Z, Fan L, Lu Y, Mao J, Huang L, Zhou J. TESN: transformers enhanced segmentation network for accurate nanoparticle size measurement of TEM images. Powder Technol 2022; 407: 117673. doi:10.1016/j.powtec.2022.117673.
[20] Okunev AG, Mashukov MY, Nartova AV, Matveev AV. Nanoparticle recognition on scanning probe microscopy images using computer vision and deep learning. Nanomaterials 2020; 10(7): 1285. doi:10.3390/nano10071285.
[21] Kharin AY. Deep learning for scanning electron microscopy: synthetic data for the nanoparticles detection. Ultramicroscopy 2020; 219: 113125. doi:10.1016/j.ultramic.2020.113125.
[22] Genc A, Marlowe J, Finzel J, Christopher P. AI-enhanced nanoparticle analysis: integrating single-shot object detection and vision transformer for rapid and accurate characterization. Microsc Microanal 2024; 30(S1): 1595-1596. doi:10.1093/mam/ozae044.196.
[23] Thuan ND, Cuong HM, Nam NH, Huong NTL, Hong HS. Morphological analysis of Pd/C nanoparticles using SEM imaging and advanced deep learning. RSC Adv 2024; 14: 35172-35183. doi:10.1039/D4RA06113F.
[24] Marsh BP, Chada N, Sanganna Gari RR, Sigdel KP, Gaffney KJ, Provost CR, Gage DJ, Craig SL, Bianculli RH, Doughty RB, Ros R. The Hessian blob algorithm: precise particle detection in atomic force microscopy imagery. Sci Rep 2018; 8(1): 978. doi:10.1038/s41598-018-19379-x. [web:123]
[25] Bright DS, Steel EB. Two-dimensional top hat filter for extracting spots and spheres from digital images. J Microsc 1987; 146(2): 191-200. doi:10.1111/j.1365-2818.1987.tb01340.x. [web:124][web:127]
[26] Boiko DA, Pentsak EO, Cherepanova VA, Ananikov VP. Electron microscopy dataset for the recognition of nanoscale ordering effects and location of nanoparticles – Dataset 1 (ordered). Figshare 2020. doi:10.6084/m9.figshare.11783661.
[27] Pedregosa F, Varoquaux G, Gramfort A, et al. Scikit-learn: machine learning in Python. J Mach Learn Res 2011; 12: 2825-2830.
[28] Vincent L. Morphological grayscale reconstruction in image analysis: applications and efficient algorithms. IEEE Trans Image Process 1993; 2(2): 176-201. doi:10.1109/83.217222.
[29] Zheng J, Hryciw RD. Segmentation of contacting soil particles in images by modified watershed analysis. Comput Geotech 2016; 73: 142-152. doi:10.1016/j.compgeo.2015.11.025.
[30] Lindeberg T. Scale-space theory in computer vision. Dordrecht: Kluwer Academic Publishers; 1994. doi:10.1007/978-1-4757-6465-9.
[31] Marr D, Hildreth E. Theory of edge detection. Proc R Soc Lond B Biol Sci 1980; 207(1167): 187-217.
[32] Kashin AS, Boiko DA, Ananikov VP. Neural network analysis of electron microscopy video data reveals the temperature-driven microphase dynamics in the ions/water system. Small 2021; 17(12): 2007726. doi:10.1002/smll.202007726. [web:128]
[33] Lunts AL, Brailovskii VL. Estimation of features obtained in statistical recognition procedures. Izv Akad Nauk SSSR Ser Tekh Kibern 1969; 3: 3-12.
[34] Kurbakov MY, Sulimova VV, Kopylov AV, Seredin OS, Boiko DA, Pentsak EO, Cherepanova VA, Ananikov VP. Determining the orderliness of carbon materials with nanoparticle imaging and explainable machine learning. Nanoscale 2024; 16(32): 13663-13676. doi:10.1039/D4NR00952E.

## *Author's information*

**Mikhail Yurievich Kurbakov** completed Bachelor's (2019) and Master's (2021) degrees in Computer Science and Engineering from Tula State University (TSU). Currently, he is a postgraduate student at TSU with a degree in Mathematical and Software Support of Computing Systems, Complexes and Computer Networks and works as a junior researcher at the Laboratory of Cognitive Technologies and Simulating Systems (LCTSS), TSU. He is the author of more than 20 scientific papers and a number of application software. E-mail: *muwsik@mail.ru*

**Valentina Vyacheslavovna Sulimova** holds a Ph.D. in Theoretical Foundations of Computer Science from the Computing Center of the Russian Academy of Sciences, Moscow, Russia, in 2009. Currently, she is an Associate Professor at the Institute of Applied Mathematics and Computer Science, TSU, and is a Senior Researcher at the LCTSS, TSU. Her research interests include data mining, pattern recognition, machine learning, signal and image analysis, supercomputing technologies. She is a member of the International Association for Pattern Recognition (IAPR), a member of the reviewer board for SN Computer Science Journal and an expert of the Russian Science Foundation. Prof. Sulimova has authored more than 80 scientific papers in refereed journals and conference proceedings on machine learning, pattern recognition and supercomputing technologies. E-mail: vsulimova@yandex.ru

**Oleg Sergeevich Seredin** holds a Ph.D. in Theoretical Foundations of Computer Science from the Computing Center of the Russian Academy of Sciences, Moscow, Russia, in 2001. Currently, he is an Associate Professor at the Institute of Applied Mathematics and Computer Science, TSU, and is a Leading Researcher at the LCTSS, TSU. His research interests include data mining, pattern recognition, machine learning, signal and image analysis, visual representation of multidimensional data, and statistical methods for decision making. Prof. Seredin has served on the program committee of many conferences (CloudCom, AIST, GraphiCon, VISAPP, PSBB, PRIB, MaDaIn). He is also member of the reviewer board for several journals, such as Sensors, Computer Optics, SN Computer Science Journal, IEEE Signal Processing Letters, Applied Science. He has worked as a visiting researcher at Rutgers University and National Taipei University of Technology. Prof. Seredin has authored more than 100 scientific papers in refereed journals and conference proceedings on machine learning, pattern recognition, and computer vision. He is a member of the IAPR. E-mail: oseredin@yandex.ru

**Andrei Valerievich Kopylov** received the Ph.D. degree from the Institute of Control Sciences of the Russian Academy of Sciences, Moscow, Russia, in 1997. Currently, he is an Associate Professor with the Institute of Applied Mathematics and Computer Science, TSU. Since 2022, he is also a Leading Researcher in the LCTSS, TSU. He worked as visiting researcher at the Dorodnicyn Computing Centre of Russian Academy of Sciences and National Taipei University of Technology. His scientific interests are signal and image analysis, data mining, machine learning. He is a member of program committee at several conferences (CloudCom, PSBB, SoICT, AIST, GraphiCon, VISAPP, ICPR), reviewer of scientific journals Sensing and Imaging, Computer Optics, Machine Learning and Data Analysis, IEEE Signal Processing Letters, IEEE Transactions on Circuits and Systems for Video Technology, IEEE Access, etc. He has published more than 100 scientific papers in refereed journals, handbooks, and conference proceedings in the areas of machine learning, pattern recognition and computer vision. Prof. Kopylov is a member of the IAPR. E-mail: and.kopylov@gmail.com

*Received September 11, 2025. The final version – November 18, 2025.*